DEGRADATION OF GRAPHITE/EPOXY COMPOSITE MATERIALS
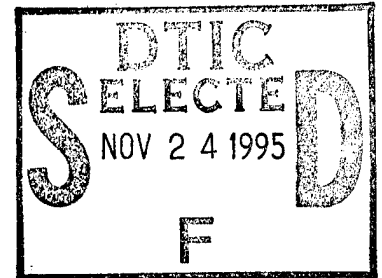## BECAUSE OF LOAD INDUCED MICROMECHANICAL DAMAGE

by

G. C. Grimes* and Dr. J. M. Whitney**

1974

ABSTRACT

Coupons axially loaded beyond a critical stress level induce permanent micromechanical damage which results in subsequent loading degradation. This phenomena will be shown for static tension, static compression, and tensile fatigue types of loading. Such observations are accurate for larger structural elements where edge effects are not significant. Where they are, the results will be low (conservative) as size goes up. Therefore, relating observed damage to failure criteria and structural design is a reasonable and safe operation.

1. INTRODUCTION

Classically in metallic technology, limit design strength has been associated with the yield strength (0.2% strain plastic deformation) and ultimate design strength with ultimate strength for static loads with some additional consideration being imposed for fatigue sensitive applications. This paper addressees the problem of determining both limit and ultimate design strengths for fiber reinforced polymeric matrix composite materials. In order to define such design strengths, it is necessary to determine stress levels in laminates at which significant damage occurs in addition to ultimate strength. Significant damage is defined as the stress level within a composite specimen at which physical damage and/or degradation of mechanical properties are initiated such that the material resistance to subsequent loadings is seriously impaired. Such mechanical properties include elastic modulus, static strength, and fatigue life.

In the determination of damage, particular attention is given to the effect of individual ply failure on the mechanical response of laminates; i.e., from an engineering point of view, does first ply failure constitute laminate failure. Individual ply failure is defined in terms of in-plane, through cracks which would cause failure if the material were not an integral part of the laminate.

The experimental results indicate that, in the absence of significant biaxial data, first ply failure provides a reasonable initial choice for limit design strength in some cases and ultimate design strength in others. It depends on whether first ply failure is caused by exceeding the 0° ply or 90° ply allowable and the application.

*SwRI
**AFML

2. MAXIMUM STRAIN CRITERION

As shown in Reference 1 the maximum strain criterion is referred to the principal lamina axes. Thus, there are three strain components which must be considered individually with respect to this criterion, i.e., lamina failure is assumed to occur if one of the following statements is satisfied:

$$\epsilon_1 = \bar{\epsilon}_1 \tag{1}$$

$$\epsilon_2 = \bar{\epsilon}_2 \tag{2}$$

$$\delta_{12} = \bar{\delta}_{12} \tag{3}$$

where ϵ is strain, 1, denotes the axis parallel to the fibers, 2 denotes the axis transverse to the fibers, and a bar signifies failure values as determined from experiments on a unidirectional material.

As previously mentioned this criterion is used to describe laminate failure as occurring when one lamina fails. Generally such lamina fails in tension by matrix cracking or fiber tensile fracture; in compression by matrix yield or tensile fracture; or as fiber compression fracture or microbuckling; and in shear by yielding for cracking of matrix.

Matrix cracking occurs because of principal stresses induced in a lamina perpendicular to its fiber direction. When such stresses cause transverse strain in excess of the lamina strain capability, the matrix breaks or yields. Such micromechanical damage does not necessarily cause ultimate failure under static conditions, but it may be the cause of fatigue failures which exceed this stress value. The phenomena was observed by Grimes, et al., in Reference 2 with further elaboration in Reference 4 by Grimes and Whitney and Grimes again in Reference 3.

In Reference 4, the point was made that failures of composite material structures under load are either matrix-controlled or filament-controlled and that such failures can be related to the lamina principal axis strength values. This is done through the use of a maximum strain criterion failure surface which will be developed in the following paragraphs.

Utilizing the standard coordinate system and notation of Reference 5 (Ashton, et al.), the stress-strain relationship of a generally orthotropic lamina is given by the stiffness matrix:

$$\begin{bmatrix} \sigma_x \\ \sigma_y \\ \tau_{xy} \end{bmatrix}^k = \begin{bmatrix} \bar{Q}_{11} & \bar{Q}_{12} & \bar{Q}_{16} \\ \bar{Q}_{12} & \bar{Q}_{22} & \bar{Q}_{26} \\ \bar{Q}_{16} & \bar{Q}_{26} & \bar{Q}_{66} \end{bmatrix}^k \begin{bmatrix} \epsilon_x \\ \epsilon_y \\ \gamma_{xy} \end{bmatrix} \tag{4}$$

where $\bar{Q}_{ij}$ are reduced stiffnesses for plane stress. The formulas necessary for the calibration of these values are given in Table I. For a unidirectional material $\bar{Q}_{16}$ and $\bar{Q}_{26}$ disappear if the principal directions 1 and 2 are taken as parallel and perpendicular to the fiber direction. The x and y then become 1 and 2, respectively.

By selecting lamina ultimate strength values for those properties which are linear to failure and proportional limit strength values for those properties which are nonlinear above this point,

2

TABLE I. TRANSFORMED LAMINA STIFFNESS MATRICES

$$\bar{Q}_{11} = U_1 + U_2 \cos(2\theta) + U_3 \cos(4\theta)$$

$$\bar{Q}_{22} = U_1 - U_2 \cos(2\theta) + U_3 \cos(4\theta)$$

$$\bar{Q}_{12} = U_4 - U_3 \cos(4\theta)$$

$$\bar{Q}_{66} = U_5 - U_3 \cos(4\theta)$$

$$\bar{Q}_{16} = -\frac{1}{2} U_2 \sin(2\theta) - U_3 \sin(4\theta)$$

$$\bar{Q}_{26} = -\frac{1}{2} U_2 \sin(2\theta) + U_3 \sin(4\theta)$$

where

$$U_1 = \frac{1}{8}(3Q_{11} + 3Q_{22} + 2Q_{12} + 4Q_{66})$$

$$U_2 = \frac{1}{2}(Q_{11} - Q_{22})$$

$$U_3 = \frac{1}{8}(Q_{11} + Q_{22} - 2Q_{12} - 4Q_{66})$$

$$U_4 = \frac{1}{8}(Q_{11} + Q_{22} + 6Q_{12} - 4Q_{66})$$

$$U_5 = \frac{1}{8}(Q_{11} + Q_{22} - 2Q_{12} + 4Q_{66})$$

where

$$Q_{11} = E_{11}/(1 - \nu_{12}\nu_{21})$$

$$Q_{22} = E_{22}/(1 - \nu_{12}\nu_{21})$$

$$Q_{12} = \nu_{21}E_{11}/(1 - \nu_{12}\nu_{21}) = \nu_{12}E_{22}/(1 - \nu_{12}\nu_{21})$$

$$Q_{66} = G_{12}$$

a set of lamina properties based on linear behavior is established. A similar set of linear behavior reduced design allowable values could also be selected if desired. It will be necessary to obtain longitudinal and transverse lamina tension and compression strength values and a shear strength value to use here. This approach works for the HY-E-1317B* graphite/epoxy laminates used herein which exhibit linear lamina stress-strain behaviors in all modes to failure except edgewise shear, which is highly nonlinear, and transverse compression, which is slightly nonlinear. Typical unidirectional stress-strain behavior is shown in Figure 1 for this material system. The longitudinal and transverse tension curves are obtained from flat tensile coupons which are straight-sided with adhesive bonded load tabs of glass reinforced epoxy laminate. Tubular specimens tested in torsion are one inch inside diameter with approximately 0.04-inch wall thickness. Fiber volume percent is approximately 60.

Average experimental strengths are tabulated in Table II. Selecting the normalized experimental (N.E.) values gives:

Tension ksi	Compression ksi	Shear ksi
$\bar{\sigma}_1 = 182.72$	$\bar{\sigma}_1 = -129.95$	$\bar{\tau}_{12} = \pm 1.47$
$\bar{\sigma}_2 = 5.47$	$\bar{\sigma}_2 = -14.40$	

A similar set of linear behavior allowable strength values (D.A.) could also be selected from Table II, if desired.

The strain-stress relations of a homogeneous orthotropic unidirectional lamina are defined by the compliance matrix as

$$\begin{bmatrix} \epsilon_1 \\ \epsilon_2 \\ \gamma_{12} \end{bmatrix} = \begin{bmatrix} S_{11} & S_{12} & 0 \\ S_{12} & S_{22} & 0 \\ 0 & 0 & S_{66} \end{bmatrix} \begin{bmatrix} \sigma_1 \\ \sigma_2 \\ \tau_{12} \end{bmatrix} \tag{5}$$

where S_{ij} values are defined in Reference 5 and shown in Table III. Moving the basic material elastic constants, the S_{ij} values can be calculated and the strain values which correspond to the
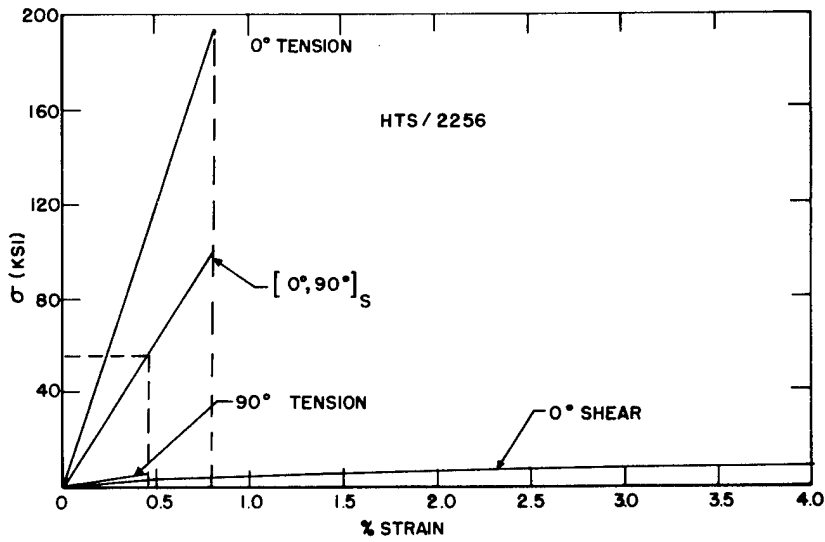
*HTS/2256.

3
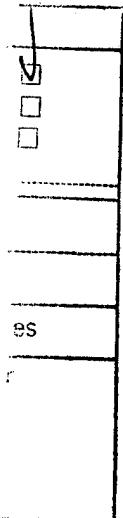
FIGURE 1. STRESS-STRAIN BEHAVIOR OF UNIDIRECTIONAL
GRAPHITE/EPOXY

properties selected above can be calculated for the four failure surface quadrants at zero shear. In addition, the pure shear strain values can be calculated with the components of the compliance matrix being:

$$S_{11} = 4.31 \times 10^{-8}$$
$$S_{22} = 73.52 \times 10^{-8}$$
$$S_{12} = -1.47 \times 10^{-8}$$
$$S_{66} = 121.95 \times 10^{-8}$$

TABLE II. GRAPHITE EPOXY LAMINA PROPERTIES*
(HTS/2256)

Type value[a]	$+\sigma_1$, ksi	$-\sigma_1$, ksi	$+\sigma_2$, ksi	$-\sigma_2$, ksi	$\pm\tau_{12}$, ksi	$+E_{11}, -E_{11}$, 10^6 psi	$+E_{22}, -E_{22}$, 10^6 psi	$\pm G_{12}$, 10^6 psi	$+\nu_{12}$ $+\nu_{21}$
N.E.–P.L.	—	—	—	14.40	1.47	23.21	1.36	0.82	0.342
–ULT.	182.72	129.95	5.47	24.67	11.30	—	—	—	0.0211 —
D.A. (R)–P.L.	—	—	—	13.06	1.16	23.21	1.36	0.82	0.342
–ULT.	164.26	97.22	4.66	21.95	8.91	—	—	—	0.0211 —
D.A. (C)–P.L.	—	—	—	7.78	0.90	23.21	1.36	0.82	0.342
–ULT.	135.00	67.14	3.51	13.36	6.90	—	—	—	0.0211 —

*Based on Reference 1 data.
Notes: Ply Thickness = 0.00841 in., Density = 0.0571 lbs/in.³ 60% F.V., 1% V.V.

TABLE III. COMPONENTS
OF THE LAMINA COM-
PLIANCE MATRIX

$$S_{11} = 1/E_{11}$$

$$S_{22} = 1/E_{22}$$

$$S_{12} = -\nu_{12}/E_{11} = -\nu_{21}/E_{22}$$

$$S_{66} = 1/G_{12}$$

$$S_{16} = S_{26} = 0$$

These values may now be used in maximum strain criterion to obtain the permissible lamina and laminate loads and stresses. From Equation (5) and these S_{ij} values, the maximum average experimental strains can be calculated and the following values obtained:

---

[a]N.E.–Normalized experimental
  D.A. (R)–Design Allowable (Realistic), based on 90% confidence level.
  D.A. (C)–Design Allowable (Confidence limit based), based on 90% lower confidence limit.

Tension-Tension Quadrant (0-shear)
$\bar{\epsilon}_1 = 7,875 \times 10^{-6}$ in./in.
$\bar{\epsilon}_2 = 4,021 \times 10^{-6}$ in./in.

Tension-Compression Quadrant (0-shear)
$\bar{\epsilon}_1 = 7,875 \times 10^{-6}$ in./in.
$\bar{\epsilon}_2 = -10,587 \times 10^{-6}$ in./in.

Compression-Compression Quadrant (0-shear)
$\bar{\epsilon}_1 = -5,601 \times 10^{-6}$ in./in.
$\bar{\epsilon}_2 = -10,587 \times 10^{-6}$ in./in.

Compression-Tension Quadrant (0-shear)
$\bar{\epsilon}_1 = -5,601 \times 10^{-6}$ in./in.
$\bar{\epsilon}_2 = 4,021 \times 10^{-6}$ in./in.

The governing constitutive equations for a homogeneous anisotropic laminate of symmetric construction subjected to in plane loadings are given by the extensional stiffness matrix of Reference 5 as:

$$
\begin{bmatrix} N_x \\ N_y \\ N_{xy} \end{bmatrix} = \begin{bmatrix} A_{11} & A_{12} & A_{16} \\ A_{12} & A_{22} & A_{26} \\ A_{16} & A_{26} & A_{66} \end{bmatrix} \begin{bmatrix} \epsilon_x^o \\ \epsilon_y^o \\ \gamma_{xy}^o \end{bmatrix}
\tag{6}
$$

where

$$
A_{ij} = \sum_{k=1}^{n} (\bar{Q}_{ij})_k \, (h_k - h_{k-1})
$$

or in more convenient form:

$$
\begin{bmatrix} \bar{\sigma}_x \\ \bar{\sigma}_y \\ \bar{\tau}_{xy} \end{bmatrix} = \begin{bmatrix} Q_{11}^* & Q_{12}^* & Q_{16}^* \\ Q_{12}^* & Q_{22}^* & Q_{26}^* \\ Q_{16}^* & Q_{26}^* & Q_{66}^* \end{bmatrix} \begin{bmatrix} \epsilon_x^o \\ \epsilon_y^o \\ \gamma_{xy}^o \end{bmatrix}
\tag{7}
$$

where

$$
\bar{\sigma}_x = \frac{N_x}{h}, \ \bar{\sigma}_y = \frac{N_y}{h}, \ \bar{\tau}_{xy} = \frac{N_{xy}}{h} \ \text{and} \ Q_{ij}^* = \frac{1}{h} \int_{-h/2}^{h/2} \bar{Q}_{ij} d_z
$$

For uniaxial tensile loading in the x-direction of symmetric composites in which the in-plane stiffness matrix is orthotropic (i.e., $A_{16} = A_{26} = 0$), the constitutive equations of Equation (6) in inverted form became

$$
\epsilon_x^o = \bar{S}_{11} N_x, \ \epsilon_y^o = \bar{S}_{12} N_x, \ \gamma_{xy}^o = 0
\tag{8}
$$

where $\bar{S}_{ij}$ are elements of the inverse matrix of Q_{ij}^* and are given by

$$
\bar{S}_{11} = \frac{Q_{22}^*}{(Q_{11}^* Q_{22}^* - Q_{12}^{*2})}, \ \bar{S}_{12} = -\frac{Q_{12}^* \bar{S}_{11}}{Q_{22}^*}
$$

Using Equation (8) in conjunction with the standard strain transformation equations yields the following relationships for applying maximum strain criterion:

$$\sigma_o^* = \frac{\bar{\epsilon}_1}{(m^2 \bar{S}_{11} + n^2 \bar{S}_{12})} \tag{9}$$

$$\sigma_o^* = \frac{\bar{\epsilon}_2}{(m^2 \bar{S}_{12} + n^2 \bar{S}_{11})} \tag{10}$$

$$\sigma_o^* = \frac{\bar{\gamma}_{12}}{2mn(\bar{S}_{11} - \bar{S}_{12})} \tag{11}$$

where

$$\sigma_o^* = \bar{\sigma}_x = \text{constant}$$

$$m = \cos \theta$$

$$n = \sin \theta$$

First ply* or ultimate* failure corresponds to the lowest value of σ_o^* as determined from Equations (9-11) using the appropriate maximum strain value.

For pure shear loading of symmetric orthotropic laminates, Equation (7) can be written in the form of

$$\bar{\tau}_{xy} = \text{constant} = \tau_o^* = Q_{66}^* \gamma_{xy}^o \tag{12}$$

or in the inverse form

$$\gamma_{xy}^o = \bar{S}_{66} \tau_o^* \tag{13}$$

where

$$\bar{S}_{66} = \frac{1}{Q_{66}^*}$$

Equation (13) in conjunction with the standard strain transformation equations yields the following relationships for applying maximum strain criterion:

$$\tau_o^* = - \frac{\bar{\epsilon}_1}{mn\bar{S}_{66}} \tag{14}$$

$$\tau_o^* = \frac{\bar{\epsilon}_2}{mn\bar{S}_{66}} \tag{15}$$

$$\tau_o^* = \frac{\bar{\gamma}_{12}}{(m^2 - n^2)\bar{S}_{66}} \tag{16}$$

*These are two different values.

6

Again the lowest value of τ_o^* as determined from Equations (14-16) correspond to the first ply or ultimate failure, depending on the maximum strain value used.

After ultimate failure is reached in a lamina, the ply is assumed to unload through a steep negative tangent modulus. Total laminate failure is assumed to occur when the Q_{ij}^* matrix becomes singular or when a negative sign appears on the diagonal. This is the same procedure used by Petit and Waddoups in Reference 6.

In Reference 4, this approach was checked against experimental data for $[0/90]_C$ and $[\pm45]_C$ laminates of HTS/ERL-2256 graphite/epoxy material. Comparison of the computed strengths based on maximum strain criterion with experimentally measured values is given in Table IV for these orientations. Correlation is reasonable.

TABLE IV. COMPARISON OF PREDICTED AND EXPERI-
MENTAL LAMINATE STRENGTH PROPERTIES
(Graphite/Epoxy: HTS[a]/ERL-2256[b])[c]

Type of value	General orientation code			
	$[0/90]_C$[d]		$[\pm45]_C$	
	Predicted	Experimental	Predicted	Experimental
Tension—P.L., psi	49,668	46,050	10,324	9,070
—ULT, psi	97,274	74,230	---	19,900
Compression—P.L.	69,185	62,210	14,381	10,150
—ULT.	—	84,070	---	22,200
Shear—P.L.	1,470	1,180	---	---
—ULT	13,400	23,400	47,975	---

Notes: F.V. = 60%
V.V. = 1%
Density = 0.0571 lbs/in.³
Ply thickness = 0.0084 in.
Meter length fiber

[a]Hercules, Inc. tradename.
[b]Union Carbide tradename.
[c]Material form: Prepreg prepared by Fiberite Corp. and designated HY-E-1317B.
[d]Based on Reference 2 data.

The proportional limit values (predicted and experimental) in tension and compression for the $[0/90]_C$ laminates of Table IV represent known significant damage levels (see Reference 2). The proportional limit value for the $[\pm45]_C$ laminates and those in shear for the $[0/90]_C$ laminates represent expected points of micromechanical damage based on these maximum strain theory predictions.

3. SIGNIFICANT DAMAGE STRESS LEVELS IN LAMINATES

The $[0/90]_C$ laminate properties and allowables shown in Table V were based on experimental data stress-strain curves. Typical curves and related cross-section photomicrographs

7

are shown in Figures 2 through 10. The G_{xy} values of Table V were measured from the small initial straight line portion of the shear stress-strain curve and may therefore be unduly high.

TABLE V. GRAPHITE/EPOXY [0/90]$_C$ LAMINATE
PROPERTIES (HTS/2256)

Ply Thickness = 0.0084 in., Density = 0.0571 lbs/in.^{3}
60% F.V., 1% V.V.

Type Values	$+\sigma_x$, $+\sigma_y$ ksi	$-\sigma_x$, $-\sigma_y$ ksi	$\pm\tau_{xy}$ ksi	E_x, E_y 10^6 psi	G_{xy}^* 10^6 psi	ν
N.E.-P.L.	46.05	62.21	1.18	13.37	1.96	0.0505
-ULT.	74.23	84.07	23.40	–	–	–
D.A.(R)-P.L.	42.00	60.20	1.10	13.37	1.96	0.0505
-ULT.	67.69	81.84	21.90	–	–	–
D.A.(C)-P.L.	31.35	58.00	0.95	13.37	1.96	0.0505
-ULT.	50.40	78.68	18.80	–	–	–

*May be too high because of measurement inaccuracy on small initial straight line portion of shear stress strain curve (see Figure   ).

The tensile coupon stress strain curve shown in Figure 2 for a [0/90]$_S$ coupon has distinct knee in the transverse strain curve at 56 ksi. Tensile specimens from this panel were loaded to stresses below and above this point, unloaded, sectioned, and studied microscopically. Photomicrographs of a specimen preloaded (but not failed) to a stress level of 43 ksi is shown in Figure 3. No damage is evident. Another specimen was preloaded (but not failed) to a stress level of 64.5 ksi, sectioned and studied microscopically. Figure 4 presents the longitudinal and transverse cross-section photomicrographs, showing cracks in the loaded longitudinal sections running through the 90° plies, perpendicular to the specimen thickness and load direction. The preload stress-strain curve on this specimen showed a transverse strain knee at 50 ksi.

Compression coupons* (utilizing platen supports) with edge gages showed knees in both the longitudinal and transverse strain curves at just under 55 ksi as shown in Figure 5. Figure 6 shows the cross-section photomicrographs of a specimen loaded in compression to a stress of 56.2 ksi, but not failed. No damage is evident. However, another specimen was loaded to the same stress level and the microscopic examination revealed a crack in one of the 0° lamina running partially across the width of the specimen (Fig. 7). An incremental compression load test to failure on a similar specimen is shown in Figure 8. While the final strength was not reduced, a knee was observed on the fifth and sixth (final) cycles which resulted in a significant modulus reduction.

A typical tube compression test* result is shown in Figure 9 illustrating a substantial deviation from linearity in the stress-strain curve between 50 and 60 ksi. A typical tube
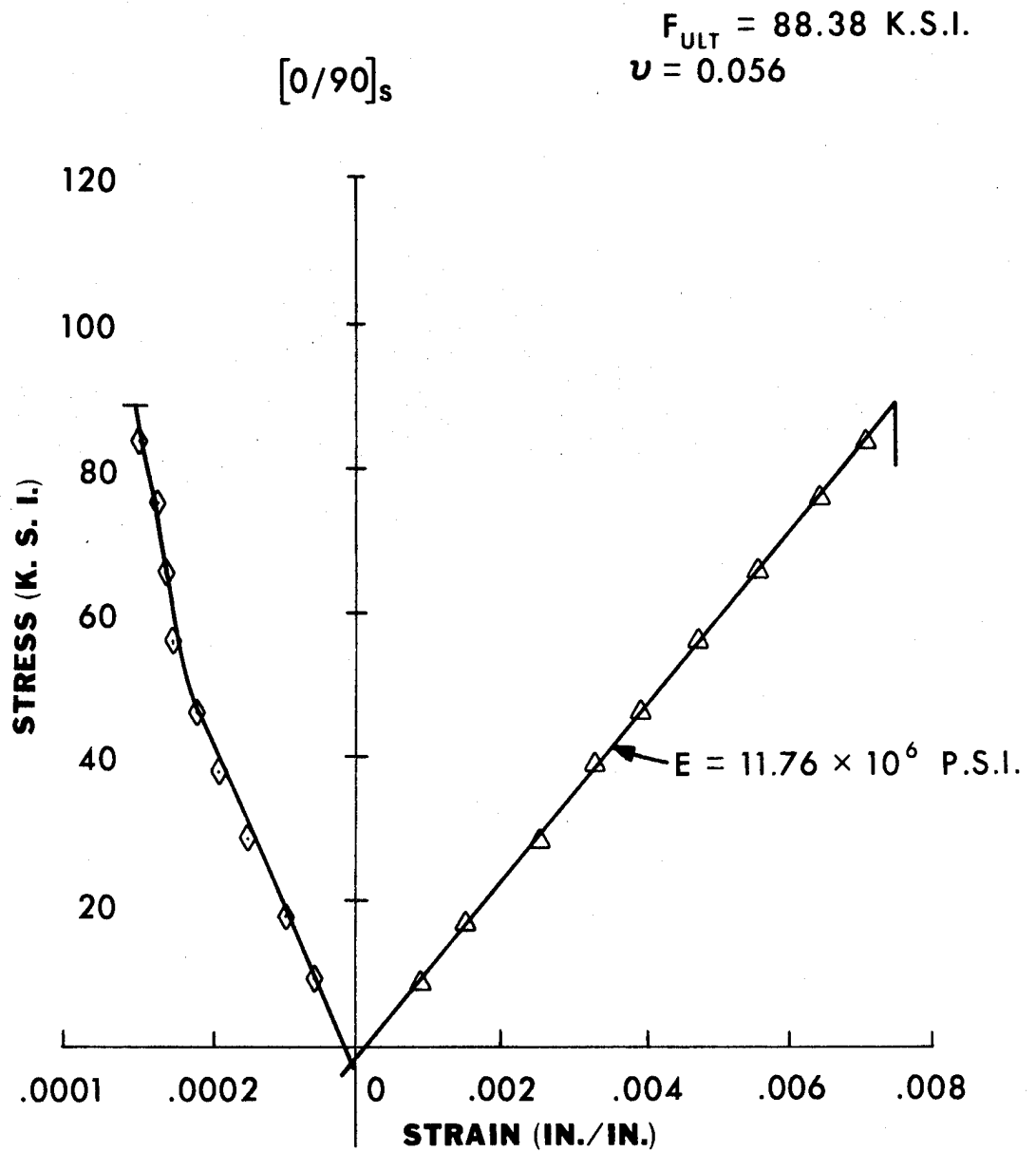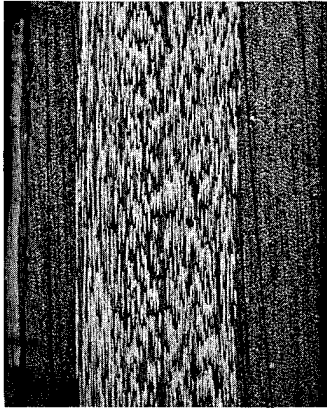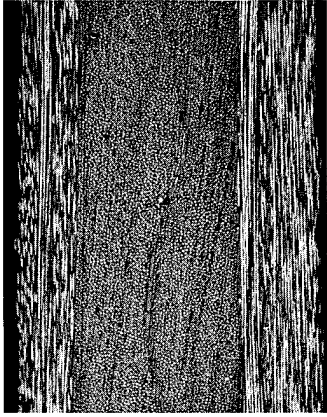
*[0/90$_2$/0]$_{2T}$

F_{ULT} = 88.38 K.S.I.

υ = 0.056

$[0/90]_s$

E = 11.76 × 10^6 P.S.I.

STRESS (K. S. I.)

STRAIN (IN./IN.)

FIGURE 2. TYPICAL STRESS VS STRAIN (TENSION)

9

B. Transverse Cross-Section—100X

A. Longitudinal Cross-Section—100X
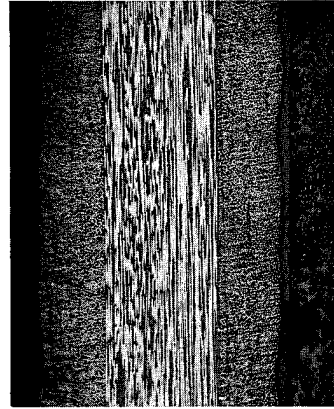
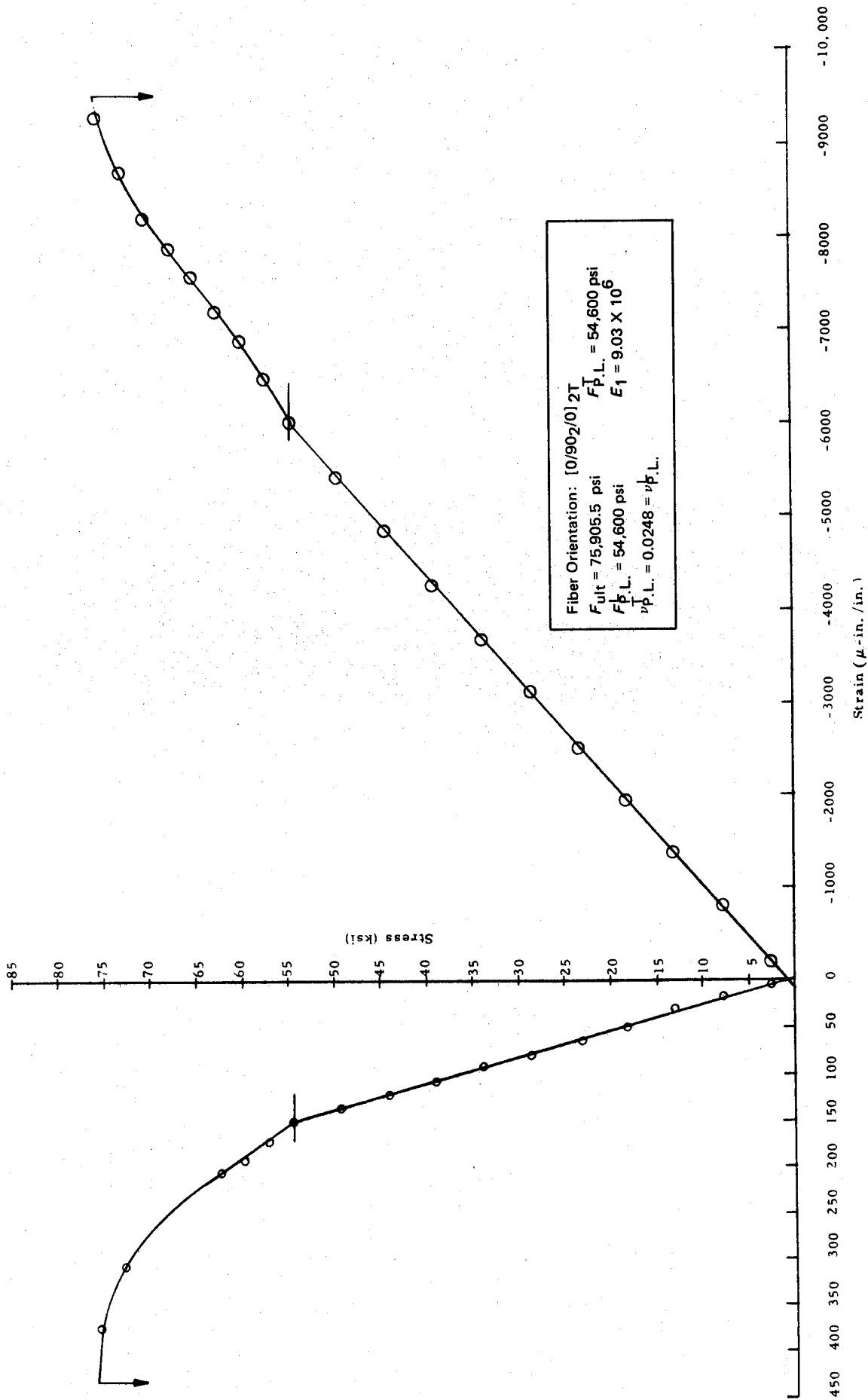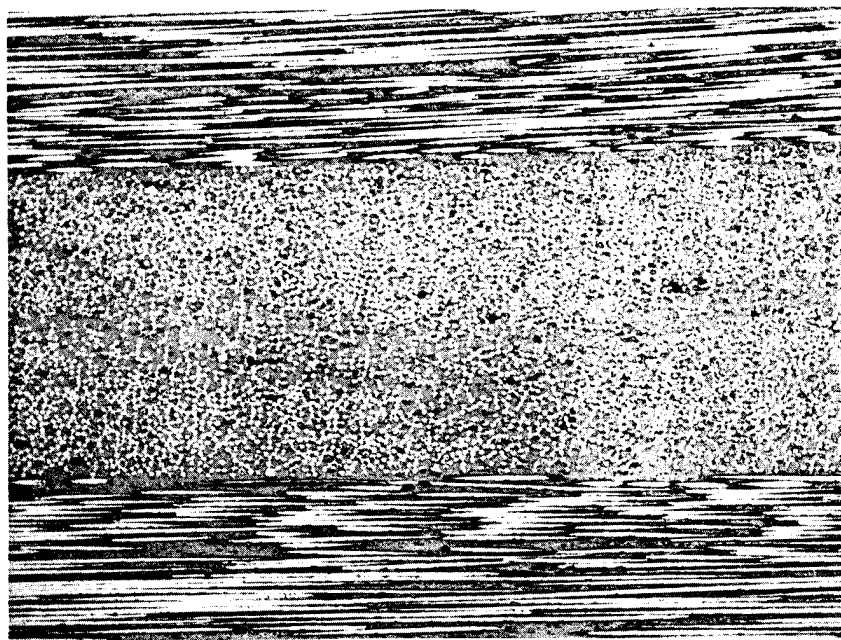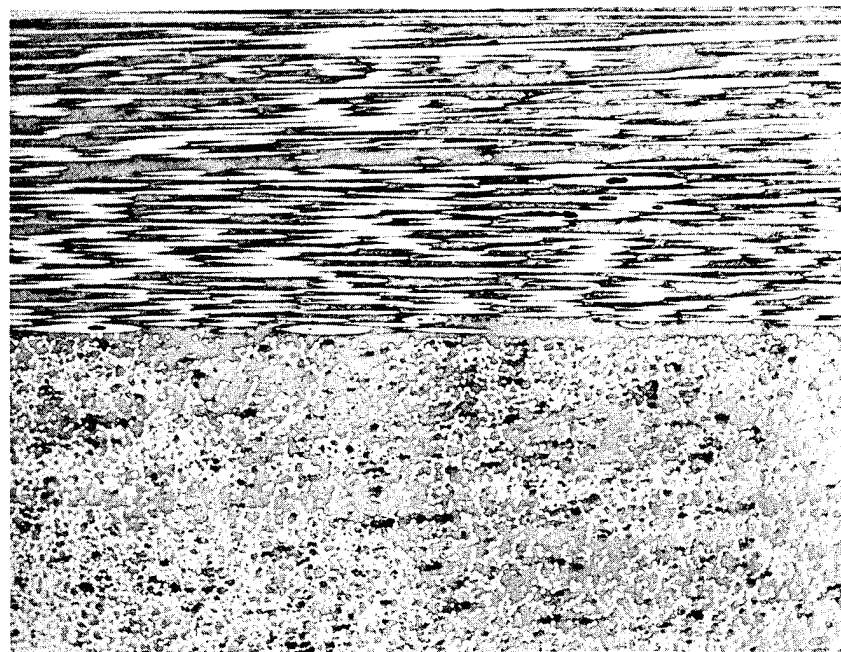FIGURE 3. PHOTOMICROGRAPHS OF SPECIMEN PRELOADED TO 43 KSI

B. Longitudinal Cross-Section—100X

A. Transverse Cross-Section—75X

FIGURE 4. PHOTOMICROGRAPHS OF SPECIMEN PRELOADED TO 64.5 KSI

10

Stress (ksi)

Strain (μ-in./in.)

Fiber Orientation: $[0/90_2/0]_{2T}$
$F_{ult} = 75,905.5$ psi
$F^T_{P.L.} = 54,600$ psi
$F^C_{P.L.} = 54,600$ psi
$\nu^C_{P.L.} = 0.0248 = \nu_{P.L.}$
$E_1 = 9.03 \times 10^6$

FIGURE 5. SPECIMEN NO. C-89-7

A. Longitudinal Cross-Section (100X)−15,
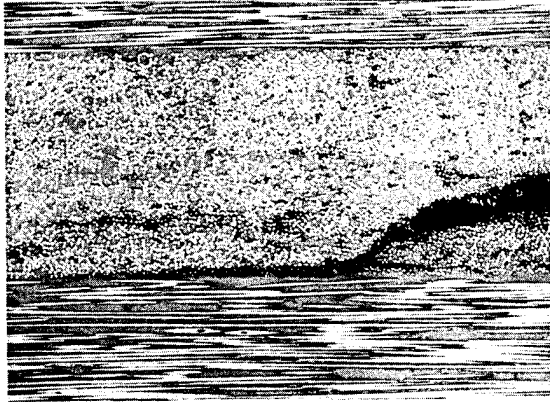No Cracks

B. Transverse Cross-Section (100X)−16,
No Cracks

FIGURE 6. PHOTOMICROGRAPHS OF PRELOADED
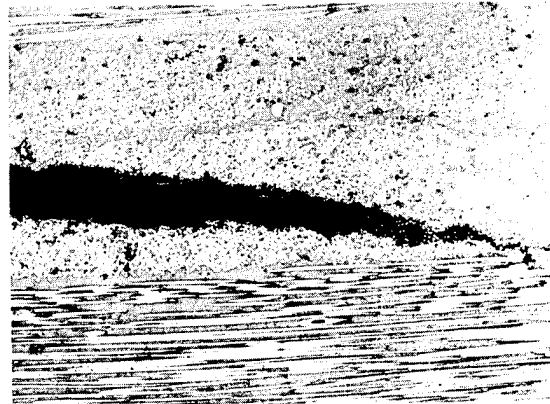COMPRESSION SPECIMEN
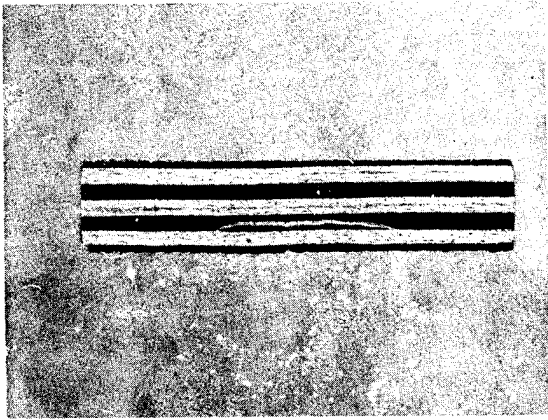
A. Transverse Cross-Section (8X)—20
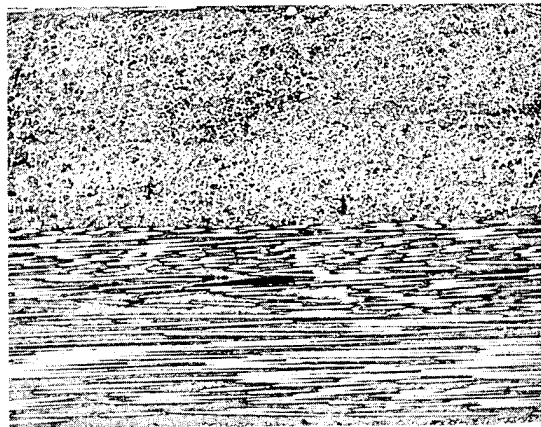Showing Whole Crack
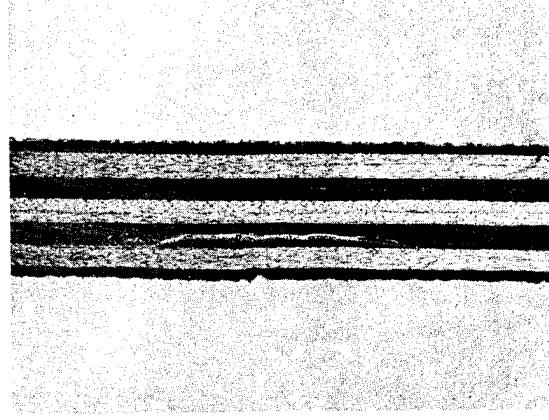
B. Transverse Cross-Section (10X)—15377
Showing Whole Crack

C. Transverse Cross-Section (100X)—19
at Left Crack Tip

D. Transverse Cross-Section (100X)—18
at Right Crack Tip

E. Longitudinal Cross-Section (100X)—17,
No Cracks

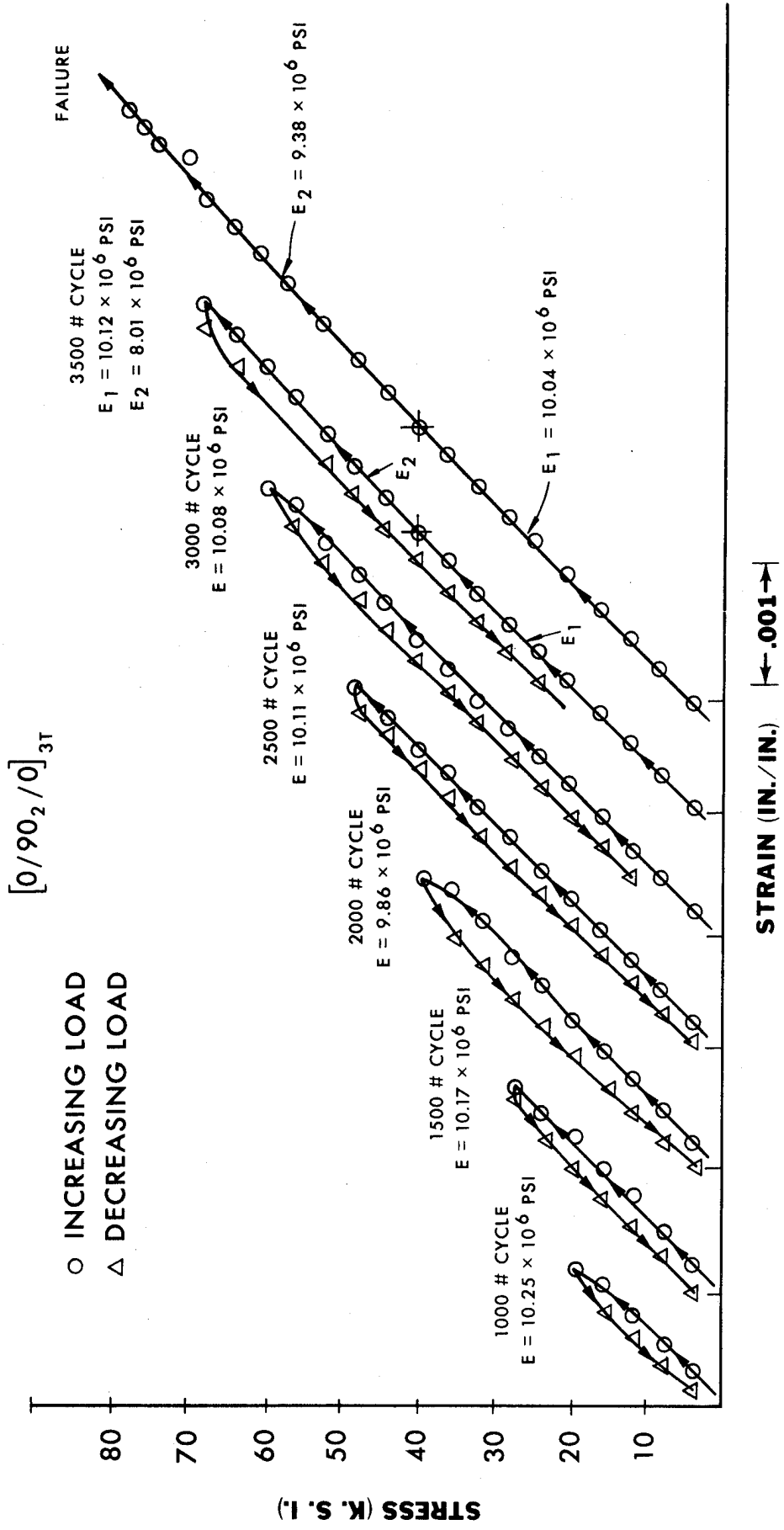FIGURE 7. PHOTOMICROGRAPHS OF PRELOADED COMPRESSION SPECIMEN

FIGURE 8. CONSECUTIVE INCREMENTAL LOADING STRESS VS STRAIN (COMPRESSION)
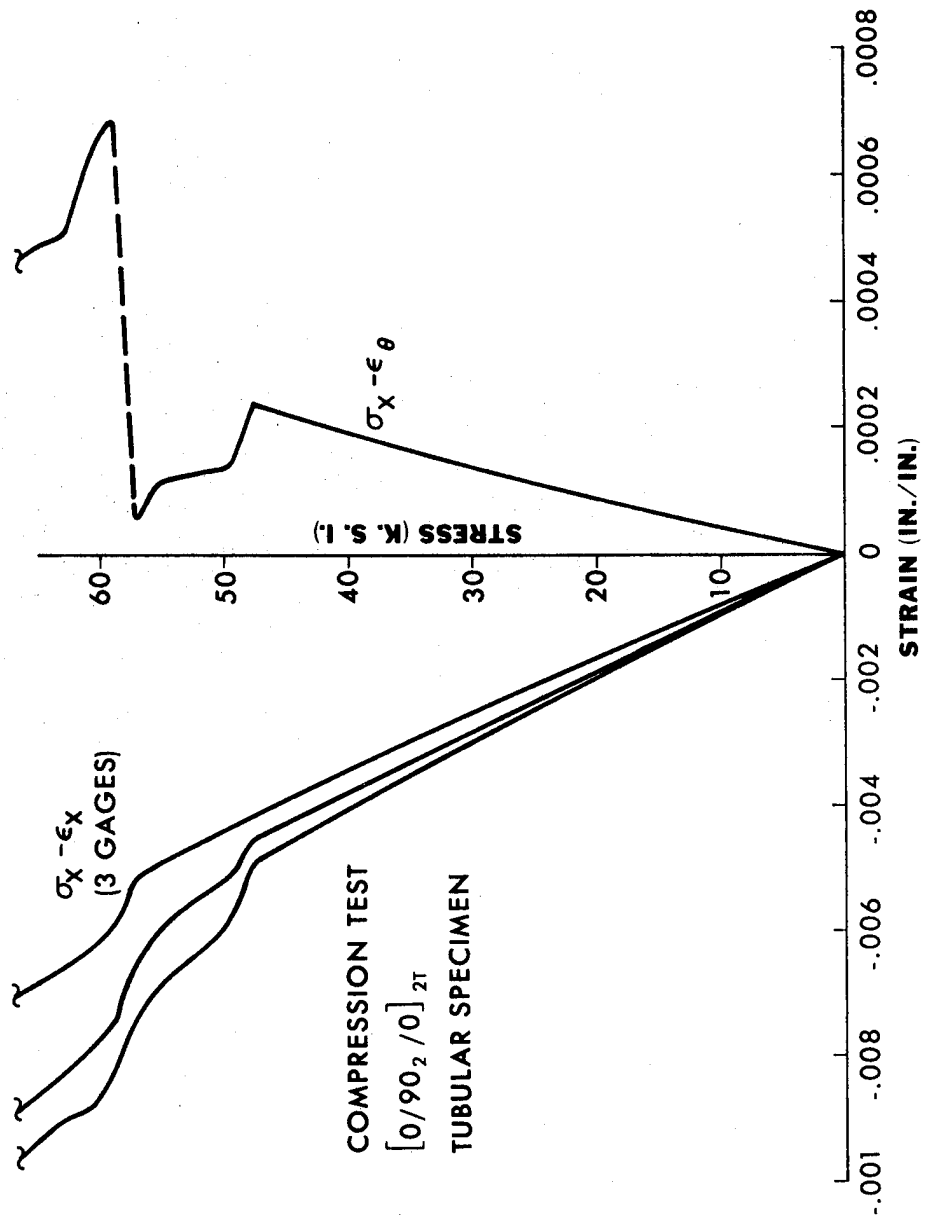
14

FIGURE 9. TYPICAL STRESS-STRAIN CURVE

torsion test result is shown in Figure 10 graphically describing the high degree of nonlinearity occurring.

The effects of the tensile damage, discussed earlier, are much more dramatic, however. Figure 11 shows the effects on the platen supported coupon compression strength, if it is first loaded in tension above the tension damage level. Apparently the 90° lamina cracking results in less 0° intralaminar strength and stability, causing progressively lower compressive failure stresses as the prior loading tensile stress level is increased.

In the context of the present paper, however, significant damage rather than ultimate strength is of prime concern. Since first ply failure is defined in terms of physical damage, which is in fact observable in the case of bidirectional graphite/epoxy laminates, it provides the starting point for assessing significant damage.

4. TENSILE FATIGUE, DAMAGE, AND RESIDUAL STRENGTH

Fatigue data generated were plotted, resulting in the curves shown in Figure 12 illustrating how the different orientations behave in fatigue and how specimen heating due to internal friction above +5°F modifies the results. Runout was considered to have occurred at from 10 to 50 million cycles, depending on the orientation. Note that the $[90/0]_c$ four- and eight-ply thick orientations have 10-million cycle runouts at 45 percent F_{TU} whereas the same thickness $[0/90]_c$ orientations have 10-million cycle runouts at 50 percent F_{TU} although the difference may not be significant. The $[0/\pm45/0]_c$ orientation (in 4 ply) run out at 50 percent F_{TU}, also, but at 50 million cycles. The twelve-ply thick $[0/90]_c$ orientations, however, run out at approximately 30 percent F_{TU} at 10 million cycles.* Microscopic study of specimen failures shows that all $[0/90]_c$ and $[90/0]_c$ orientations had cracking of the 90° plies, causing delamination and 0° ply overload and tensile failure. The $[0/\pm45/0]_c$ specimen appeared to fail either by edge effects (see Reference 7) or 45° ply failure at 90° to the fibers. The cracking and failure of 90° ply due to its strain incompatability with plies of other orientations (especially 0°) appear to be a phenomena separate and distinct from the edge effects observed in Reference 7. Thus, the 90° ply cracking has the effect of putting a limited, measurable life on these materials.

Those specimens tested that did not fail were subsequently tested in static tension to failure in order to measure residual strength. Some increased scatter is evident in these residual strength specimens when compared with original static strength specimens. Such data will be of interest in reliability analysis.

5. RESULTS AND CONCLUSIONS

A. Maximum Strain Criterion

Maximum strain criterion has been developed and shown to be an accurate prediction technique for determining both the ultimate and significant damage (proportional limit) stress levels of $[0]_C$, $[0/90]_C$, and $[\pm45]_C$ orientations of graphite/epoxy laminates under axial and shear loading. Therefore, first ply failure provides a reasonable choice for limit

---

*This lower value may be caused by the inefficiency of the bonded load introduction tabs on thicker laminates.
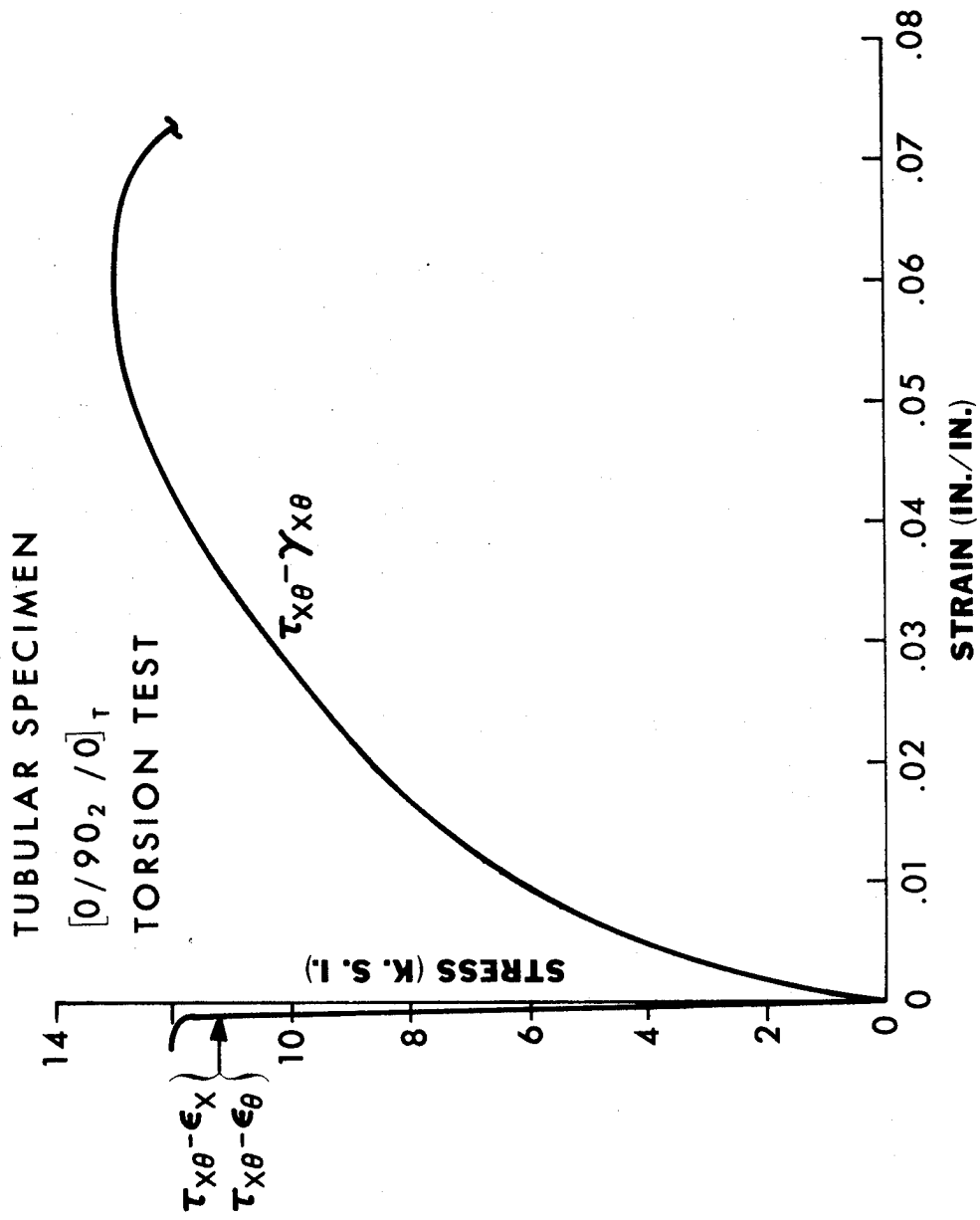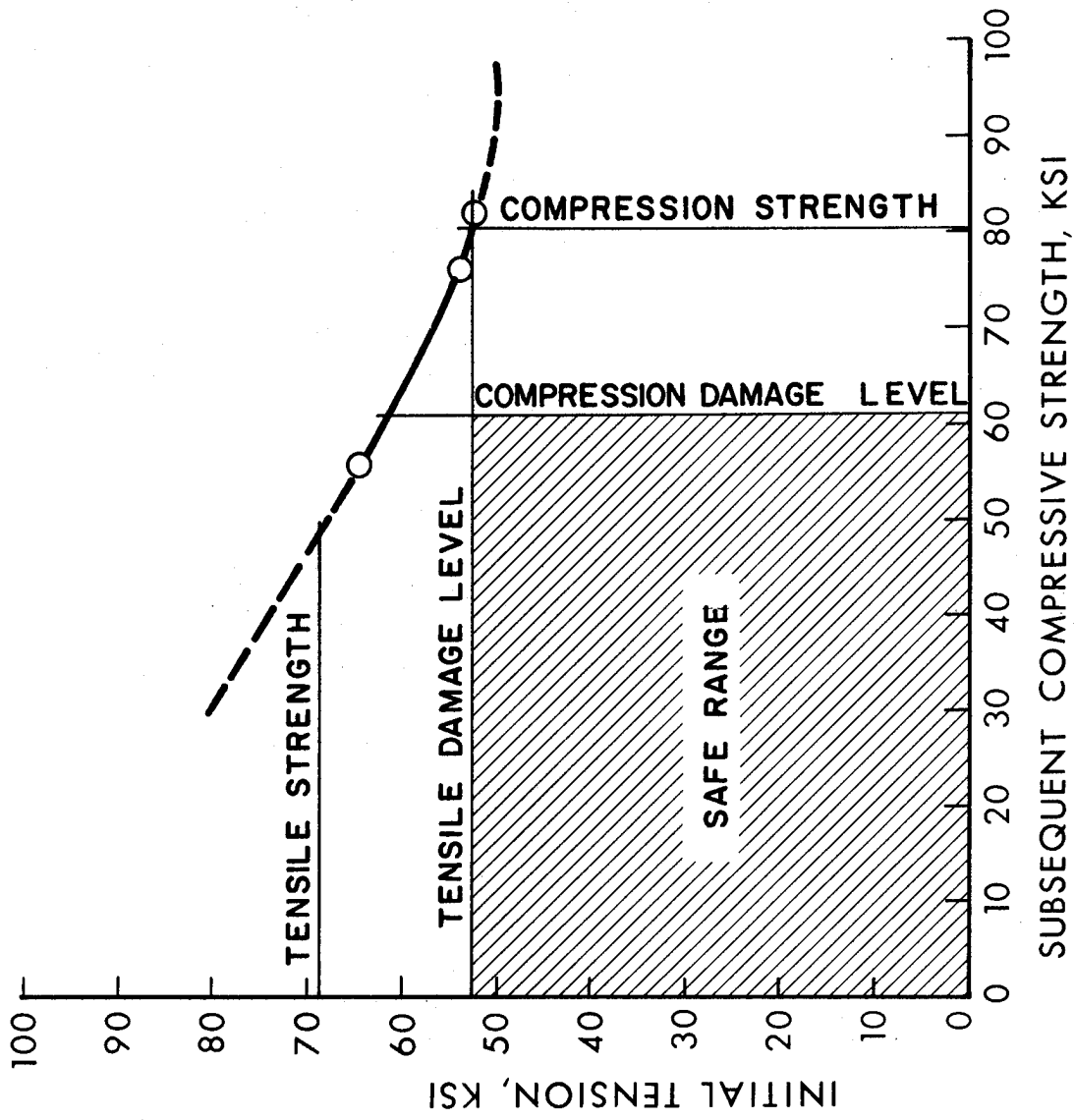
FIGURE 10. STRESS-STRAIN CURVE

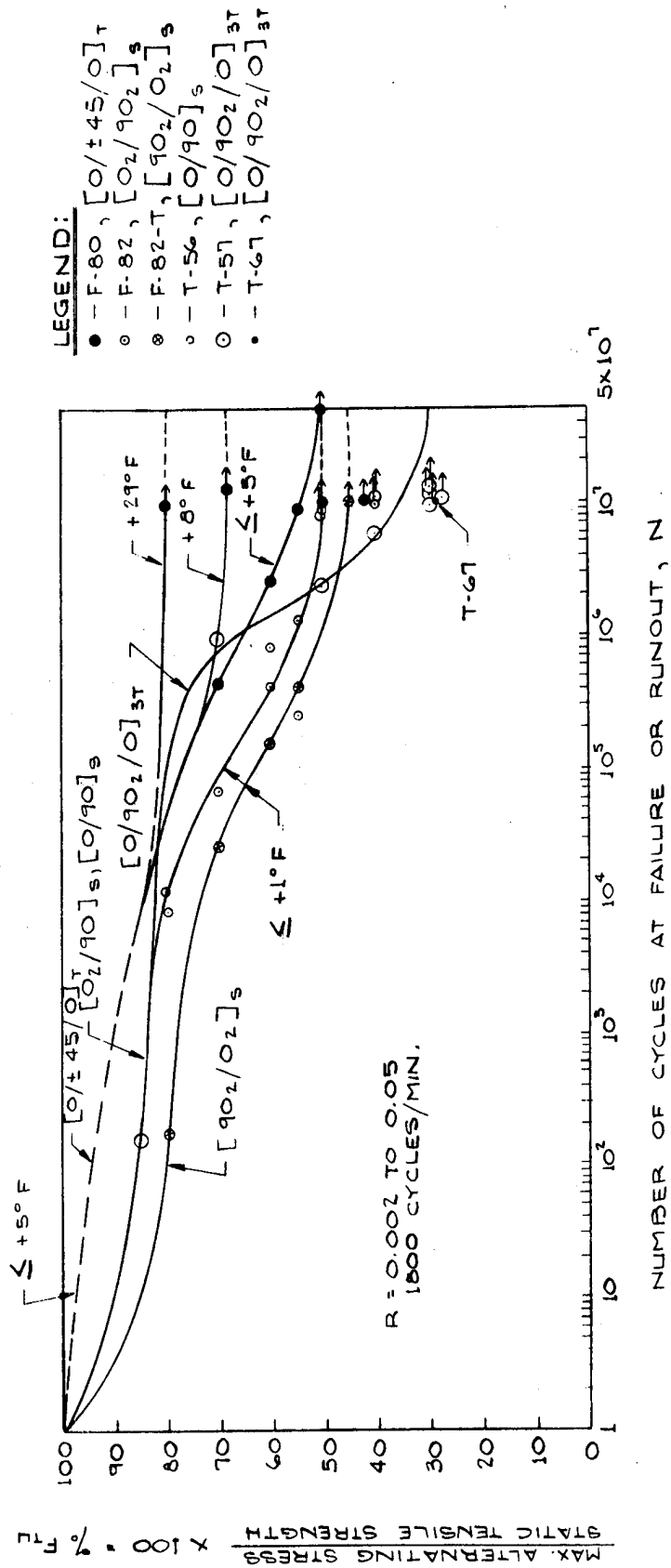FIGURE 11. INITIAL-TENSION.SUBSEQUENT COMPRESSION
CHARACTERISTICS

FIGURE 12. GRAPHITE EPOXY %F$_{TO}$-N TENSILE FATIGUE CURVE
(2256/M$_1$L$_1$-HTS)

19

and/or ultimate design strength.* While there is some indication that this criterion works for the [0]$_C$ and [0/90]$_C$ orientations under biaxial loading (see Reference 1), this area needs further verification.

Such conclusions emphasize, as discussed in detail by Halpin,[8] the importance of a balance of ply properties when considering the potential of a given composite material for wide structural application. It should be noted that these conclusions only pertain to polymeric matrix composites. For metal matrix materials in which the basic stress-strain response involves significant yielding, the damage level and type may be quite different.

B. Observation of Experimental Behavior Under Static Loading

Two significant damage stress levels were observed in the [0/90]$_C$ laminates under axial loading. In tension the 90° ply, transverse to the thickness, cracking at 62.0% of the ultimate laminate strength† was found to correspond to the [90]$_C$ lamina strain at its ultimate failure stress. In compression the 0° ply longitudinal cracking partially across the width of the laminate specimen, occurs at approximately 72% of the ultimate strength. The specimen strain level at which this 0° ply significant damage in compression occurs is roughly equal to the [0]$_C$ lamina compressive strain at its experimental ultimate failure stress.‡

The tensile damage level stress was identified by a knee in the longitudinal stress/transverse strain curve and visually verified by microscopic observation of the resulting 90° ply cracks which constitute significant micromechanical degradation. This tensile damage shows up (1) in subsequent tensile loading Poisson's ratio values which are lower, (2) in reduced subsequent loading compression strength, and (3) in tensile fatigue (endurance limit) strengths which are less than or equal to the damage level stress. The compression damage level stress was identified by knees in both the longitudinal and transverse strain curves and by sectioning specimens after they were progressively loaded to higher stresses but not failed. The transverse sections revealed cracking in the 0° plies at approximately the 72% of ultimate strength level. Another property change noticed as a result of this micromechanical damage was when specimens were subjected to periodically increasing incremental compressive loadings until failure occurred. On the first cycle after the damage level stress was reached or exceeded there was a knee in the longitudinal compressive stress-strain curve with knees in each of the succeeding cycle stress-strain curves to failure. The resulting secondary modulus was significantly reduced compared with the primary one. Tube compressive tests on [0/90]$_C$ materials also exhibited knees on both the longitudinal and transverse strain curves at stress values slightly above 70% ultimate but at strain levels which were close to the [0]$_C$ lamina experimental strain levels at ultimate failure (as measured herein on flat specimens).

C. Shear

Because significant yielding is associated with shear loads on polymeric materials, the shear stress-strain curve in Figure 10 is highly nonlinear. Such behavior is likely to cause significant interaction between shear and normal loads, resulting in a breakdown of the maximum strain criterion. In structural applications such extreme departure from linear elastic behavior is not permissible. As a result, allowable shear strains are not permitted to exceed

*Depending on whether it's 0° or 90° ply failure and upon the application.
†The 62% F$_{TU}$ value is the average of both 4-ply and 12-ply panels. The 90° ply damage point on 4-ply specimens was at a lower percent of F$_{TU}$ than on the 12-ply specimens, although the strain levels were approximately the same.
‡As measured on an 8-ply, 0° specimen made and tested in the platen supported jig. This represents the onset of intralaminar tension failure; short column compressive strength is estimated to be approximately 20-25% higher.

1%-1-1/2%. In such a case, the interactions between shear and normal loads are likely to be minimized, permitting maximum strain to again be a useful tool for predicting first ply failure and laminate damage. But, the prediction of ultimate strength may require more sophisticated approaches.[9,10]

D. Fatigue

Fatigue results indicate that micromechanical damage resulting from the maximum alternating stresses exceeding the significant damage level do cause fatigue failures at lifetimes far short of the defined endurance limit. It appears that for most orientations of this graphite/epoxy material, the endurance limit (whether it be 10 or 50 million cycles) strength is in the neighborhood of 50 percent of static F_{TU} for tension-tension constant cycle fatigue. Strength scatter of unfailed fatigue specimens is greater than that of virgin static test values.

ACKNOWLEDGEMENT

REFERENCES

1. Whitney, J. M., Browning, C. E., and Grimes, G. C., "The Relationship Between Significant Damage and the Stress-Strain Response of Laminated Polymeric Matrix Composites," May 1972, ASM Publication.

2. Grimes, G. C.; Francis, P. H.; Commerford, G. E.; Wolfe, G. K., "An Experimental Investigation of the Stress Levels at Which Significant Damage Occurs in Graphite Fiber Plastic Composites," AFML-TR-72-40, May 1972.

3. Grimes, G. C., "Analysis of Discontinuities, Edge Effects, and Joints," a chapter in the book **Structural Analysis and Design** by C. C. Chamis. A volume in the **Treatise on Composite Materials**, edited by Brontman and Krock; to be published by Academic Press in 1974.

4. Grimes, G. C. and Whitney, J. M., "The Relationship Between Design Allowables and Load-Induced Micromechanical Damage in Composite Materials," **Colloquium on Structural Reliability: The Impact of Advanced Materials on Engineering Design**, Carnegie Mellon University, October 1972.

5. Ashton, J. E.; Halpin, J. C.; and Petit, Ph. H., **Primer on Composite Materials: Analysis**, Technomic Co., 1969.

6. Petit, P. H. and Waddoups, M. E., "A Method of Predicting the Nonlinear Behavior of Laminated Composites," *Journal of Composite Materials*, 3, pp. 2-19, January 1969.

7. Piper, R. B., "Interlaminar Stresses in Composite Laminates," AFML-TR-72-18, May 1972.

8. J. C. Halpin, "Structure-Property Relations and Reliability Concepts," *Journal of Composite Materials*, Vol. 6, April 1972, pp. 208-231.

9. A. K. Malmeister, "Geometry of Theories of Strength," *MEKHANIKA POLIMEROV*, Vol. 2, No. 4, 1966, p. 519; English Translation: *Polymer Mechanics*, Vol. 2, No. 4, 1966, p. 324, pub. Faraday Press.

10. S. W. Tsai and E. M. Wu, "A General Theory of Strength for Anisotropic Materials," *Journal of Composite Materials*, Vol. 5, January 1971, pp. 58-81.